

sections 1-2 and 3-4 of the pipeline (see Fig. 1); c , mass concentration of solution; h , head loss in converging section, mm H₂O gage; Δh_{1-2} and Δh_{3-4} , head losses in sections 1-2 and 3-4, respectively; α_D , α_d and v_D , v_d , corrections for the kinetic energy and mean velocity of the flow in the pipe sections of diameters D and d ; g , acceleration of free fall; $Re = v_d d / \nu$, Reynolds number; ν , kinematic viscosity; λ , hydraulic friction coefficient for pipe; ζ , resistance coefficient of converging section; ζ_B , ζ_{π} , resistance coefficients during the flow of water and of aqueous PAA solution; $\Delta\zeta/\zeta = 100\%$, $(\zeta_B - \zeta_{\pi})/\zeta_B$ relative change in the coefficient ζ caused by the introduction of the PAA additive to the stream under otherwise equal flow conditions.

LITERATURE CITED

1. L. P. Kozlov, *Visn. Akad. Nauk URSR*, No. 1, 23-33 (1987).
2. I. L. Povkh, *Visn. Akad. Nauk URSR*, No. 11, 66-74 (1982).
3. B. V. Lipatov, *Izv. Akad. Nauk SSSR, Mekh. Zhidk. Gaza*, No. 2, 153-155 (1974).
4. V. B. Amfilokhiev, *Tr. Leningrad. Korablastroist. Inst.*, No. 89, 7-11 (1974).
5. I. L. Povkh and V. V. Chernyuk, *Inzh.-Fiz. Zh.*, 51, No. 3, 357-361 (1986).
6. V. V. Chernyuk, *Special Problems of the Hydraulics and Purification of Natural and Waste Waters [in Russian]*, Deposited in UkrNIINTI on August 27, 1985, No. 1964, L'vov (1985).
7. V. V. Chernyuk, *Vestn. L'vov. Politekh. Inst.*, No. 208, 79-82 (1986).

CONJUGATE HEAT TRANSFER IN THE LAMINAR FLOW OF A SWIRLED INCOMPRESSIBLE FLUID IN A HORIZONTAL ANNULAR DUCT

V. I. Bubnovich and P. M. Kolesnikov

UDC 536.242:532.542.2

The heat transfer associated with swirled flow of a heat-transfer medium in a semi-infinite annular duct is analyzed numerically. The walls of the duct have a finite thickness and exert a significant influence on the formation of the temperature fields in the fluid.

The swirling of flow in ducts, annular ducts in particular, is widely employed in engineering as an effective means of intensifying heat- and mass-transfer processes, stabilizing plasmas and flames, and protecting the walls of equipment against high-temperature and chemically aggressive flows. The types of swirled flow are extremely diverse: completely and partially swirled flows, flows with local and constant swirling along the length (ducts fitted with augers, helical liners and windings, etc.), flows in septate and conical ducts, etc. A detailed classification of the types of swirled flows is given in two recently published books [1, 2].

The influence of flow rotation on the velocity distribution in an annular duct and the onset of zones of flow separation from the inner wall have been investigated [3-5] over a wide range of swirling factors, Reynolds numbers, and thicknesses of the annular space. The specific characteristics of the intensification of convective heat transfer by swirled flow of a heat-transfer medium in an annular duct are discussed in [6, 7]. The main experimental and theoretical results on the hydrodynamics and heat transfer of swirled flows in axisymmetrical ducts are generalized in [2].

Lately a growing importance has been placed on the solution of both the inner and outer problems of convective heat transfer in the conjugate setting: in general, the temperature fields in the duct walls and in the fluid flow are highly interdependent, and appreciable errors can arise in thermal calculations if this coupling is ignored. Data from investiga-

A. V. Lykov Institute of Heat and Mass Transfer, Academy of Sciences of the Belorussian SSR, Minsk. Translated from *Inzhenerno-Fizicheskii Zhurnal*, Vol. 57, No. 5, pp. 713-720, November, 1989. Original article submitted May 7, 1988.

tions of the influence of the thickness and thermal conductivity of the duct walls on convective heat transfer by the swirled flow of a heat-transfer medium have not been published to date.

Here we consider the unsteady laminar flow of an incompressible fluid in a straight annular duct with flow swirling at the inlet. We assume that the flow is rotationally symmetrical, external body forces are absent, and the density ρ and dynamic viscosity coefficient μ are constant. In cylindrical coordinates the dimensionless Navier-Stokes equations for such a flow have the form [4]

$$\begin{aligned} \frac{\partial v}{\partial r} + \frac{v}{r} + \frac{\partial u}{\partial z} &= 0, \\ \frac{\partial v}{\partial t} + v \frac{\partial v}{\partial r} + u \frac{\partial v}{\partial z} - \frac{\omega^2}{r} &= -\frac{\partial P}{\rho \partial r} + \frac{1}{\text{Re}} \left(\nabla^2 v - \frac{v}{r^2} \right), \\ \frac{\partial u}{\partial t} + v \frac{\partial u}{\partial r} + u \frac{\partial u}{\partial z} &= -\frac{\partial P}{\rho \partial z} + \frac{1}{\text{Re}} \nabla^2 u, \\ \frac{\partial \omega}{\partial t} + v \frac{\partial \omega}{\partial r} + u \frac{\partial \omega}{\partial z} + \frac{v\omega}{r} &= \frac{1}{\text{Re}} \left(\nabla^2 \omega - \frac{\omega}{r^2} \right). \end{aligned} \quad (1)$$

The heat transfer in the fluid flow and in the duct walls is described by the system of differential equations

$$\frac{\partial T_2}{\partial t} + v \frac{\partial T_2}{\partial r} + u \frac{\partial T_2}{\partial z} = \frac{1}{\text{Pe}} \nabla^2 T_2, \quad \frac{\partial T_1}{\partial t} = \frac{a}{\text{Pe}} \nabla^2 T_1. \quad (2)$$

The initial and boundary conditions are:

$$\begin{aligned} T_1 = T_2 = u = v = \omega = 0 \quad \text{at} \quad t \leq 0; \quad t > 0: \quad T_1 = T_2 = v = 0, \\ u = U_0(r), \quad \omega = W_0(r) \quad \text{at} \quad z = 0, \quad \frac{\partial u}{\partial z} = \frac{\partial v}{\partial z} = \frac{\partial \omega}{\partial z} = \frac{\partial T_1}{\partial z} = \frac{\partial T_2}{\partial z} = 0 \\ \text{at} \quad z = L, \quad u = v = \omega = 0, \quad T_1 = T_2, \quad \lambda \frac{\partial T_2}{\partial r} = \frac{\partial T_1}{\partial r} \quad \text{at} \quad r = R, \quad r = R+1, \\ \frac{\partial T_1}{\partial r} = 0 \quad \text{at} \quad r = R-c, \quad \frac{\partial T_1}{\partial r} = \text{Bi}(1-T_1) \quad \text{at} \quad r = R+1+c, \end{aligned} \quad (3)$$

where $R = R_1/(R_2 - R_1)$ and c is the thickness of the duct walls.

Boundary conditions for the pressure are not formulated, because we eventually eliminate the pressure from the system of equations (1). Everything is set equal to zero in the initial conditions. The following parameters, on which the solution of the stated problem depends, are adopted: the dimensionless radius R of the inner cylinder, the dimensionless thickness c of the duct walls, the Reynolds number Re , the Péclet number Pe , the dimensionless length L of the duct, the axial and azimuthal velocity profiles U_0 and W_0 at the inlet, the ratio $a = a_1/a_2$ of the thermal diffusivities of the duct walls and the fluid, and the ratio $\lambda = \lambda_2/\lambda_1$ of the thermal conductivities of the fluid and the duct walls. We use a Poiseuille profile for U_0 and assume that the radial variation of the azimuthal velocity component at the duct inlet obeys the rigid-body law

$$W_0 = K_0 r.$$

To characterize the quantitative relation between the axial velocity u and the azimuthal velocity ω in the duct cross section, we define the quantity K by the expression

$$K(z) = \int_R^{R+1} \omega(r, z) dr \left[\int_R^{R+1} u(r, z) dr \right]^{-1}, \quad K_0 = K(0).$$

The objective of the study is to determine the dependence of the solution of the system of equations (1), (2) subject to the boundary conditions (3) on the parameters K_0 , λ , and c for large values of L .

The introduction of the stream function ψ and the azimuthal component of the vorticity ξ :

$$u = \frac{1}{r} \frac{\partial \psi}{\partial r}, \quad v = -\frac{1}{r} \frac{\partial \psi}{\partial z}, \quad \xi = \frac{\partial v}{\partial z} - \frac{\partial u}{\partial r}$$

reduces the system of equations (1) to the form

$$\frac{\partial \xi}{\partial t} + v \frac{\partial \xi}{\partial r} + u \frac{\partial \xi}{\partial z} - \frac{\xi v}{r} - \frac{1}{r} \frac{\partial \omega^2}{\partial z} = \frac{1}{\text{Re}} \left(\nabla^2 \xi - \frac{\xi}{r^2} \right), \quad (4)$$

$$\frac{\partial \omega}{\partial t} + v \frac{\partial \omega}{\partial r} + u \frac{\partial \omega}{\partial z} + \frac{v \omega}{r} = \frac{1}{\text{Re}} \left(\nabla^2 \omega - \frac{\omega}{r^2} \right), \quad (5)$$

$$\xi = -\frac{\partial}{\partial r} \left(\frac{1}{r} \frac{\partial \psi}{\partial r} \right) - \frac{1}{r} \frac{\partial^2 \psi}{\partial z^2}. \quad (6)$$

The boundary conditions for the functions ψ and ξ are obtained from conditions (3) and have the form

$$\psi = \int_R^r U_0(r) r dr, \quad \xi = -\frac{\partial U_0}{\partial r} \quad \text{at } z=0, \quad \frac{\partial \psi}{\partial z} = \frac{\partial \xi}{\partial z} = 0 \quad \text{at } z=L, \quad (7)$$

$$\psi = \frac{\partial \psi}{\partial r} = 0 \quad \text{at } r=R, \quad \psi = \int_R^{R+1} U_0(r) r dr = 1, \quad \frac{\partial \psi}{\partial r} = 0 \quad \text{at } r=R+1.$$

The vorticity boundary problems deserve special attention. The problem is that the values of the function ξ (or its derivatives) at the boundaries of the domain must be specified in order to solve the vorticity equation (4) numerically. On the other hand, the boundary conditions (7) do not contain any information in explicit form on the function ξ at the duct walls, where the no-slip condition must hold:

$$\frac{\partial \psi}{\partial r} \Big|_R = 0. \quad (8)$$

Numerical methods for the solution of the incompressible fluid equations do not permit this condition to be used directly. It is therefore necessary to derive equations that describe the vorticity function and satisfy condition (8). This is accomplished by introducing internal iterations with respect to the time step Δt for the function ξ at the boundary. The simultaneous solution of Eqs. (4) and (6) in one time step proceeds as follows in this case [8, 9]. An alternating-direction procedure is first used to solve the vorticity equation (the values of the vorticity at the walls are taken from the preceding iteration layer) and the Poisson equation in succession. The values of the stream function at nodes situated one step from the boundary of the physical domain are then adjusted for nonslip by any one-sided formula for the derivative (8), e.g. [10]:

$$\frac{\partial \psi}{\partial r} \Big|_{r_1} = \frac{-3\psi_1 + 4\psi_2 - \psi_3}{2\Delta r} + O(\Delta r^2).$$

The values of the vorticity are corrected at the same nodes according to Eq. (6), and the values of this quantity at the boundary of the domain are determined from the unsteady equation (4) expressed at near-boundary nodes. The final values of the vorticity at the boundary are determined from the relation

$$\xi_0^{n,k} = \xi_0^{n,k-1} \alpha + \xi_0^{n,k-1} (1 - \alpha),$$

in which n is the number of the time layer, k is the iteration number, and α is a relaxation parameter, which affects only the rate of convergence of the iterative process and is taken equal to 0.5 in the majority of situations. The iterative process is terminated when, e.g., the following relation is satisfied:

$$\left| \xi_0^{n,k} - \xi_0^{n,k-1} \right| / \left| \xi_0^{n,k} \right| \leq 10^{-4}.$$

The system of equations (2), (4)-(6) subject to the initial and boundary conditions (3), (7) has been solved numerically by an implicit finite-difference scheme using an alternating-direction procedure [10]. Clearly, if we introduce the fictitious time τ and transform Eq. (6) to the parabolic-type equation

$$\frac{\partial \psi}{\partial \tau} - \frac{\partial}{\partial r} \left(\frac{1}{r} \frac{\partial \psi}{\partial r} \right) - \frac{1}{r} \frac{\partial^2 \psi}{\partial z^2} = \xi, \quad (9)$$

all five equations of the basic system will have a similar structure, so that a unified

method and computational algorithm can be used to solve them. Accordingly, we give the finite-difference analog of the equation for the energy in the fluid and omit the finite-difference representations of all other equations of the system, since they can be written by analogy with the following:

$$\begin{aligned}
& \frac{\bar{T}_{ij} - T_{ij}}{\Delta t/2} + (v_{ij} + |v_{ij}|) \frac{T_{ij} - T_{ij-1}}{2\Delta r_{j-1}} + (v_{ij} - |v_{ij}|) \frac{T_{ij+1} - T_{ij}}{2\Delta r_j} + \\
& \quad + \frac{\bar{T}_{ij} - \bar{T}_{i-1j}}{2\Delta z_{i-1}} (u_{ij} + |u_{ij}|) + \frac{\bar{T}_{i+1j} - \bar{T}_{ij}}{2\Delta z_i} (u_{ij} - |u_{ij}|) = \\
& = \frac{1}{\text{Pe}} \left[r_{j+1} \frac{T_{ij+1} - T_{ij}}{r_j \Delta r_j^2} - \frac{T_{ij} - T_{ij-1}}{\Delta r_j \Delta r_{j-1}} + \frac{\bar{T}_{i+1j} - \bar{T}_{ij}}{\Delta z_i^2} - \frac{\bar{T}_{ij} - \bar{T}_{i-1j}}{\Delta z_i \Delta z_{i-1}} \right], \\
& \frac{\hat{T}_{ij} - \bar{T}_{ij}}{\Delta t/2} + (v_{ij} + |v_{ij}|) \frac{\hat{T}_{ij} - \hat{T}_{ij-1}}{2\Delta r_{j-1}} + (v_{ij} - |v_{ij}|) \frac{\hat{T}_{ij+1} - \hat{T}_{ij}}{2\Delta r_j} + \\
& \quad + (u_{ij} + |u_{ij}|) \frac{\bar{T}_{ij} - \bar{T}_{i-1j}}{2\Delta z_{i-1}} + (u_{ij} - |u_{ij}|) \frac{\bar{T}_{i+1j} - \bar{T}_{ij}}{2\Delta z_i} = \\
& = \frac{1}{\text{Pe}} \left[r_{j+1} \frac{\hat{T}_{ij+1} - \hat{T}_{ij}}{r_j \Delta r_j^2} - \frac{\hat{T}_{ij} - \hat{T}_{ij-1}}{\Delta r_j \Delta r_{j-1}} + \frac{\bar{T}_{i+1j} - \bar{T}_{ij}}{\Delta z_i^2} - \frac{\bar{T}_{ij} - \bar{T}_{i-1j}}{\Delta z_i \Delta z_{i-1}} \right], \tag{10}
\end{aligned}$$

where $\bar{T} = T^{n+1/2}$ and $\hat{T} = T^{n+1}$. Equations (10) are solved in each direction r and z by the well-known tridiagonal inversion method [11].

The temperature matching conditions at the inner and outer cylinders are transformed into the respective finite-difference equations

$$\begin{aligned}
T_{1ij} &= T_{2ij}, \frac{T_{1ij} - T_{1ij-1}}{\Delta r_{j-1}} = \lambda \frac{T_{2ij+1} - T_{2ij}}{\Delta r_j} \quad \text{at } r = R, \\
T_{1ij} &= T_{2ij}, \lambda \frac{T_{2ij} - T_{2ij-1}}{\Delta r_{j-1}} = \frac{T_{1ij+1} - T_{1ij}}{\Delta r_j} \quad \text{at } r = R + 1.
\end{aligned}$$

Equation (9) contains the relaxation parameter which has the values $\min(\Delta r_j)/5$ and $\min(\Delta z_i)/5$ in the execution of the inversion sweeps along the r and z directions, respectively.

The above-described numerical algorithm for the solution of the Navier-Stokes equations in vorticity-stream function variables has been implemented in the present study. A nonuniform 17×22 computational grid with the clustering of points near the walls and inlet to the duct was used. The convection terms in Eqs. (2), (4), and (5) were represented by asymmetric first-order difference relations with so-called "upstream orientation" [10]. The velocity fields were computed in terms of central differences, and the local Nusselt numbers $\text{Nu}(z)$ at the inner surface of the outer cylinder were determined from the relation

$$\text{Nu}(z) = \frac{\partial T}{\partial r} \Big|_{r=R+1} (T|_{r=R+1} - \bar{T})^{-1}.$$

The time step depended on the Reynolds number Re and the step of the spatial grid and varied between the limits 0.05-0.08. The computations were terminated when the following convergence test was satisfied:

$$\left| \frac{\phi^n - \phi^{n-1}}{\phi^n} \right| \leq 0.005,$$

where $\phi = (\psi, \xi, T_1, T_2, \omega)$. The relaxation time of the solution of the problem increased with the duct length L , attaining a value $t = 100$ at $L = 100$.

The reliability of the formulated algorithm was certified on the basis of published data on the hydrodynamics of swirled flow [4] and on fully developed flow in the initial thermal section of an annular duct [12]. Computations on a z -uniform, r -nonuniform 21×11 grid (21 lengthwise and 11 radially) for $\text{Re} = 10$, $R = 1$, $L = 1.2$, and $K_0 = 6$ indicated exact agreement of the results with the data of [4]; in particular, flow separation from the inner wall takes place at the inlet to the duct. As the swirl parameter K_0 is increased and the flow separation zone occupies an ever-increasing region of the fluid flow. We also investigated the variation of the frictional stress on the inner wall of the duct as the

swirl parameter K_0 was increased from 1 to 10. We observed good agreement of the results with those of similar investigations reported in [4]. Good agreement was also exhibited by the dependence of the "critical swirl" on the geometrical parameter R in the interval 0.5-4.0 and on the Reynolds number in the range from 10 to 10^3 . In testing the thermal part of the problem, we investigated the initial thermal section of a straight annular duct with hydrodynamically stabilized fluid flow and the following boundary conditions ($R = 1$):

$$T(r, 0) = 1, T(R, z) = 0, \left. \frac{\partial T}{\partial r} \right|_{r=R+1} = 0.$$

The Nusselt numbers determined from the solution of the problem

$$Nu(z) = 2 \left. \frac{\partial T}{\partial r} \right|_{r=R} \bar{T}^{-1}$$

at the inner wall of the duct are in good agreement with the corresponding data of [12], deviating at most by 7%.

The flow and heat transfer in the duct are governed by the following set of parameters: the geometrical parameters R , C , and L , the axial and azimuthal velocity profiles U_0 and W_0 at the inlet to the duct; the Reynolds number Re ; the Péclet number Pe , and the Biot number Bi ; the flow swirl factor K_0 at the inlet to the duct; and the ratios of the thermal conductivities λ and the thermal diffusivities a of the duct walls and the fluid. In our work the parameters c , K_0 , and λ were varied in order to ascertain the nature of their influence on the solution of the problems, the profiles of U_0 and W_0 are given above, and the remaining parameters are $Re = 100$, $Pe = 50$, $L = 100$, $Bi = 1$, $a = 10$, and $R = 1$.

We known [12] that heat transfer in a duct with Cauchy-type boundary conditions takes place under isothermal wall conditions in the limit $Bi \rightarrow \infty$. To test this fact in the presence of swirled flow and to confirm the reliability of the results, we carried out a corresponding investigation with the parameters $R = 1$, $K_0 = 3$, $\lambda = c = 0.05$, $a = 10$, and $Bi = 100$. A comparison of the solution obtained here with heat-transfer data in the case of Dirichlet-type boundary conditions indicates good agreement between them. It suffices to note that the comparison of the Nusselt numbers and the bulk temperatures of the fluid for both problem exhibits the greatest differences directly at the inlet to the duct, which are equal to 3.5% and 1.0%, respectively. Consequently, for $Bi = 100$ and the values given above for the other parameters of the problem, heat transfer actually takes place in the duct with Dirichlet boundary conditions. We therefore specify a much smaller value of the Biot number in the ensuing investigation, setting it equal to unity.

The variation of the Nusselt number and the bulk temperature of the fluid along the duct for various degrees of swirl is shown in Fig. 1. As the swirl parameter K_0 is increased from 0 to 10, heat transfer within the active zone of the centrifugal forces is greatly intensified; farther downstream, this effect decays rapidly until, e.g., at $z = 47.5$ the Nusselt number is equal to 2.53 for all three cases. A somewhat similar situation has been [13] in a numerical analysis of the influence of flow swirling on the heat transfer in

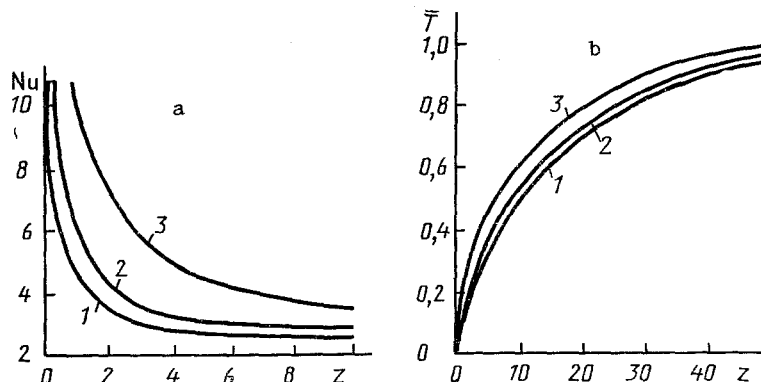


Fig. 1. Variation of the Nusselt number (a) and the bulk temperature of the fluid (b) along the duct, $c = \lambda = 0.05$. 1) $K_0 = 0$; 2) 3; 3) 10.

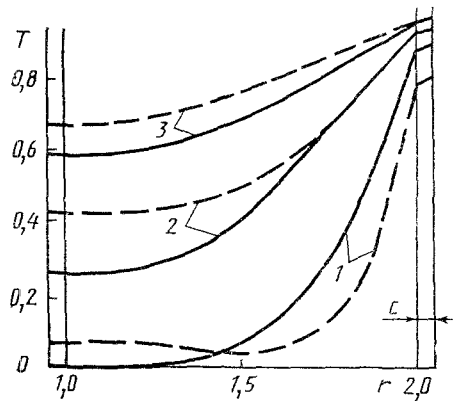


Fig. 2. Temperature distribution in different cross sections of the duct, $c = \lambda = 0.05$. 1) $z = 2.0$; 2) 10.0 ; 3) 21.25 . Swirl parameter: $K_0 = 0$ (solid curves) and $K_0 = 10$ (dashed curves).

a circular tube. In a comparison of the heat fluxes for various degrees of swirl, the authors of this work showed that in the zone of significant influence of centrifugal forces the heat flux in the fluid increases with the parameter K_0 , but the opposite effect takes place farther downstream.

The temperature distributions in different cross sections of the duct for a swirl factor of 10 and without swirl are compared in Fig. 2. We know [4] that for $Re = 100$ and $R = 1$ flow separation from the inner wall of the duct sets in at values of K_0 slightly greater than 3. In fact, our numerical experiment confirms the fact that for $K_0 = 3.3$ a weak, small-volume vortex emerges at the inner wall of the duct, and a flow-separation point occurs at $z \approx 0.5$. As the swirl factor is increased, the separation zone takes up an ever-increasing region of the flow: for $K_0 = 10$ the dimensions of the vortex formation relative to the thickness of the annular duct are equal to 0.5 and 9.0 in the r and z directions, respectively, i.e., it has a highly elongated (along z) structure, which has a strong influence on the heat transfer in the duct. Indeed, the presence of the flow separation zone in the initial section of the duct for $K_0 = 10$ causes the warmer upper layers of the fluid to be transported convectively toward the inner wall and causes the temperature minimum to shift toward the middle of the duct. The temperature profile is characterized by the presence near the wall of a distinct almost-flat interval, which represents the flow core and occupies a large part of the annular space. Here the temperature varies only slightly in the radial direction from point to point; in return, the temperature profile rises sharply upward in the vicinity of the outer wall of the duct. The influence of flow swirling gradually vanishes with increasing z (see curves 2 and 3), and the temperature minimum shifts toward the inner wall of the duct.

The influence of the other parameter of the problem — the thermal conductivity λ of the duct walls — on the heat transfer in an annular duct is illustrated by Figs. 3 and 4. We see (Fig. 3) that when λ is increased, the bulk temperature of the fluid decreases, and the Nusselt number increases within the indicated intervals of z . The formation of the temperature profiles along the entire length of the duct also depends significantly on the thermal conductivity λ of the walls (Fig. 4). However, this dependence differs in different cross sections of the duct: In the initial cross sections (curves 1) the influence of the wall material on the temperature profile is felt in the heat-emitting wall itself and in the fluid layer immediately contiguous with it; farther downstream (curves 2) this influence extends deeper and deeper into the fluid, reaching the inner thermally insulated wall, and finally at sufficiently large z the maximum temperature variations with variation of the parameter λ take place at the inner wall (curves 3).

The influence of the wall thickness on the heat-transfer characteristics in an annular duct for Cauchy boundary conditions was investigated for the parameters $R = 1$, $\lambda = 0.5$, $K_0 = 3$, and $a = 10$. The dimensionless thickness of the duct walls was varied in the interval 0.01-0.1. The investigation showed that the variations of the Nusselt numbers and the bulk temperature of the fluid in the above-indicated range of c with the values of all other

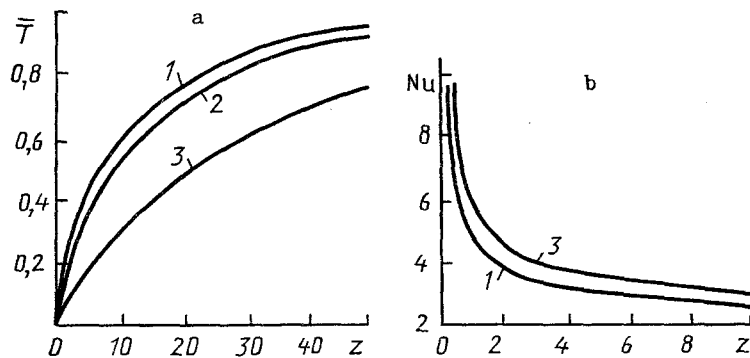


Fig. 3. Variation of the bulk temperature of the fluid (a) and the Nusselt numbers (b) along the length of the duct for various values of λ , $K_0 = 3$, $c = 0.05$. 1) $\lambda = 0.01$; 2) 0.05; 3) 0.5.

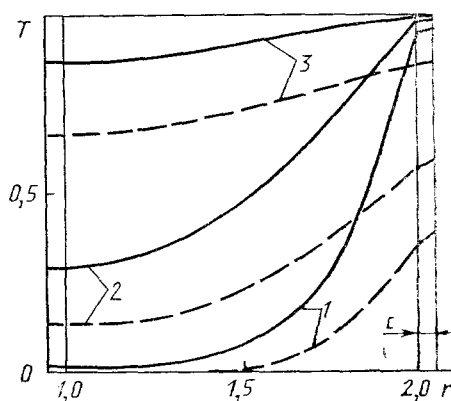


Fig. 4. Temperature distribution in different cross sections of the duct, $K_0 = 3$, $c = 0.05$. 1) $z = 2.5$; 2) 10.0; 3) 47.5. Thermal conductivity: $\lambda = 0.5$ (dashed curves) and $\lambda = 0.01$ (solid curves).

parameters fixed are so slight that they are difficult to portray graphically: in the inlet cross sections for $c = 0.01$ and $c = 0.1$ the Nusselt numbers and the bulk temperatures differed by 3% and 14%, respectively. Farther downstream, however, these differences decrease rapidly, soon becoming equal to 1% and 5% in the cross section $z = 2.0$ for the Nusselt numbers and the bulk temperature, respectively. It should also be noted that in the zone of large centrifugal forces the bulk temperature of the fluid decreases and the Nusselt numbers increase as the wall thickness is increased.

Thus, the foregoing numerical analysis shows that the duct walls play a significant role in the formulation of the temperature field of the heat-transfer medium.

NOTATION

r , z , dimensionless radial and axial coordinates; u , v , ω , dimensionless velocity components in axial, radial, and tangential directions; L , dimensionless duct length; c , dimensionless thickness of duct walls; λ_1 , λ_2 , thermal conductivities of duct walls and fluid, respectively; ξ , ψ , dimensionless vorticity and stream function; t , dimensionless time; Bi , Biot number.

LITERATURE CITED

1. V. K. Shchukin, Heat Transfer and Hydrodynamics of Inner Flows in Body-Force Fields [in Russian], Moscow (1980).
2. V. K. Shchukin and A. A. Zhalatov, Heat Transfer, Mass Transfer, and Hydrodynamics of

- Swirled Flows in Axisymmetrical Ducts [in Russian], Moscow (1982).
3. R. Z. Alimov and V. I. Luk'yanov, in: Heat and Mass Transfer in Aircraft Engines [in Russian], Kazan (1982), pp. 34-41.
 4. V. V. Tret'yakov and V. I. Yagodkin, Inzh.-Fiz. Zh., 34, No. 2, 273-280 (1978).
 5. N. F. Budunov, Izv. Sib. Otd. Akad. Nauk SSSR Ser. Tekh. Nauk, No. 13, Issue 3, 3-10 (1977).
 6. V. V. Kulalae, in: High-Temperature Gas Flows, Their Generation and Diagnostics [in Russian], No. 3 (1983), pp. 23-31.
 7. A. S. Korsun and O. V. Mitrofanova, Heat and Mass Transfer VII (collected scientific papers of the Institute of Heat and Mass Transfer, Academy of Sciences of the Belorussian SSR) [in Russian], Vol. 8, Part 1 (1984), pp. 86-91.
 8. E. F. Nogotov and A. K. Sinitsyn, Inzh.-Fiz. Zh., 31, No. 6, 1113-1119 (1976).
 9. A. G. Daikovskii, V. I. Polezhaev, and L. I. Fedoseev, Chisl. Metody Mekh. Sploshnoi Sredy, Vol. 10, No. 2, 61-66 (1979).
 10. V. M. Paskonov, V. I. Polezhaev, and L. A. Chudov, Numerical Simulation of Heat- and Mass-Transfer Processes [in Russian], Moscow (1984).
 11. A. N. Tikhonov and A. A. Samarskii, Equations of Mathematical Physics, Pergamon Press, Oxford (1963).
 12. B. S. Petukhov, Heat Transfer and Resistance in Laminar Fluid Flow in Tubes [in Russian], Moscow (1967).
 13. M. F. Shnaiderman and A. I. Ershov, Inzh.-Fiz. Zh., 28, No. 4, 630-635 (1975).

NATURAL THERMAL-CONCENTRATION CONVECTION

Yu. A. Buevich and V. N. Mankevich

UDC 536.25:541.135

Combined thermal and concentration convection is studied for the example of the problem of flow and transport near the surface of a horizontal disk.

Natural convection processes in the field of gravity are determined by the dependence of the density of the fluid on the temperature or the concentration of the impurity diffusing in it and the nonuniformity of the fields of these quantities in the presence of heat and mass transfer from surfaces immersed in the fluid. There are a very large number of studies of free-convection stimulated by only one of the indicated factors and of the corresponding convective transport processes (see the review in [1, 2]). A significant number of numerical studies of situations in which both factors are important at the same time have also been performed. Free convective flow at a horizontal surface is, however, an exception in this respect; to analyze this flow it is necessary to study not only the horizontal but also the vertical component of the vector equation of conservation of momentum. This makes the calculations significantly more complicated, which apparently explains the fact that there are only a few isolated papers on the study of such flow.

Numerical solutions, however, in spite of their importance in obtaining reliable quantitative results, are very cumbersome and, most importantly, they are not very useful for constructing a complete physical picture of the process and formulating comparatively simple relations describing the process in a wide range of values of the parameters. Attempts, of which we are aware, to describe analytically the combined thermal concentration convection (made, in particular, in the analysis of the macrokinetics of heterogeneous reactions) are, as a rule, based on the use of asymptotic boundary layer methods combined with the principle of superposition, which cannot, in principle, be correct when it is applied to strong convective heat conduction and diffusion processes [3]. Inaccuracies of a fundamental character, concerning the determination of the effective thicknesses of the hydrodynamic and thermal or diffusion layers (see below), which must be corrected, are also encountered in the use of a thin boundary layer. Finally, there are experimental indications [4] of the

A. M. Gor'kii Ural State University, Sverdlovsk. Moscow Institute of Chemical Machine Building. Translated from Inzhenerno-Fizicheskii Zhurnal, Vol. 57, No. 5, pp. 721-729, November, 1989. Original article submitted May 24, 1988.